APPLICATION OF MICROTREMOR MEASUREMENTS TO THE ESTIMATION OF SITE AMPLIFICATION CHARACTERISTICS

Mehedi A. ANSARY[1], Fumio YAMAZAKI[2] and Tsuneo KATAYAMA[3]

Introduction

Wave propagation mechanism of microtremor and its relation with ground vibration characteristics were studied from the beginning of microtremor studies (Aki, 1957; Kanai and Tanaka, 1961). Meanwhile practical application of microtremor in the field of engineering has advanced tremendously. One of the powerful and simplest application of microtremor observation is in seismic micro-zoning.

Basically there are two types of microtremor observations regarding to the number of observation points. These are point and array observations of microtremors. From the array observation of microtremor of period greater than 1s, Rayleigh-wave and Love-wave originating from natural sources, such as sea wave, variation of air and wind pressure, can be recognized. On the other hand short-period microtremor of period less than 1s is thought to be generated by artificial noises such as traffic vehicles, industrial plants, household appliances, etc. Some researchers (Sato et al., 1991; Tokimatsu and Miyadera, 1992; Tokimatsu et al., 1994) have showed that microtremors are mainly composed of fundamental mode of Rayleigh-wave and some (Nakamura, 1989; Wakamatsu and Yasui, 1995) have showed that short-period microtremor bears resemblance to shear-wave characteristics. On the other hand, microtremors can also be dominated by Love-wave (Tamura et al., 1993). Recently, Suzuki et al. (1995) have applied microtremor measurements to the estimation of earthquake ground motions based on a hypothesis that the amplitude ratio defined by Nakamura can be regarded identical with half of the amplification factor from bedrock to the ground surface. However, the real generation and nature of microtremors have not yet been established.

Microtremor observation is mainly popular in Japan as can be observed from the references of the preceding paragraph. Recently, some researchers from France and Mexico are trying to use it as a tool to predict site response (Lermo and Chavez-Garcia, 1994a), to determine site amplification characteristics using Nakamura's method to strong ground motion records (Theodulidis and Bard, 1995) and for the prediction of predominant period of a site (Lermo and Chavez-Garcia, 1994b). Lachet and Bard (1995) have justified the reliability of Nakamura's method for site effects application.

In the last few years, to cope with the secondary disasters after an earthquake, city gas companies in Japan have promoted several countermeasures: increasing seismic resistance of facilities and pipelines, segmentation of gas networks into blocks, earthquake monitoring by seismometers. For this reason, an earthquake monitoring and emergency operation system (Yamazaki et al., 1994 and Yoshikawa et al., 1995) has been developed by Tokyo Gas company. For the development of this system, ground motion amplification based on different site conditions of the network area is an important parameter. Keeping this objective in mind, short-period microtremor measurements at

1) Graduate student, Department of Civil Engineering, University of Tokyo.
2) Associate Professor, Institute of Industrial Science, University of Tokyo.
3) Professor, Institute of Industrial Science, University of Tokyo.

thirteen sites of Tokyo metropolitan area have been observed.

From the existing borelogs and PS-loggings, soil model at each site is established for theoretical analysis. The theories are based on the assumption that microtremor is composed of either Rayleigh-wave or shear-wave. Then applying Nakamura's (1989) QT-spectrum technique the amplitude ratio for microtremor observation at each site is determined. This ratio is then compared with similar theoretical amplitude ratios for Rayleigh and shear-waves obtained by using the established soil model for the site.

A parametric study of two-layer soil model is undertaken to establish the correspondence between the periods obtained from the Rayleigh and shear-waves for different impedance ratios of the soil layers. For the three microtremor array sites, the propagation velocity obtained from the frequency wave-number (F-K) spectrum analysis of the vertical motion of observed microtremors are compared with the phase velocity of the Rayleigh-wave.

Microtremor observations

The instrument used for the microtremor measurement is SPC-35T (Tokyo Sokushin Co.). The obtained velocity records by the sensors are highpass-filtered (0.1Hz) and amplified (amplifier: 8 channels) and then converted to digital recording using a 16 bits AD converter for storage in the hard disk of a personal computer. For velocity measurement, sensitivity of the instrument is flat for period less than about 1s. The observed arrays are pentagonal in shape with 3 sensors at the center: one vertical (UD) and two horizontal (NS, EW), and 5 vertical sensors (UD) arranged at five corner points of the pentagon having radius of 20m. Figure 1 shows the observed microtremor array arrangement. Microtremor observations are recorded for 2 minutes per hour at every hour for 24 hours at the six sites by using the built-in clock of the personal computer. Sampling frequency of 100Hz was used. For the rest of the sites, 3 recordings per site each with 2 minutes record size, are observed.

Table 1 presents basic information regarding the microtremor observations. The sites are generally regulator stations and gas factories. Figure 2 shows the area under study together with the location of thirteen sites.

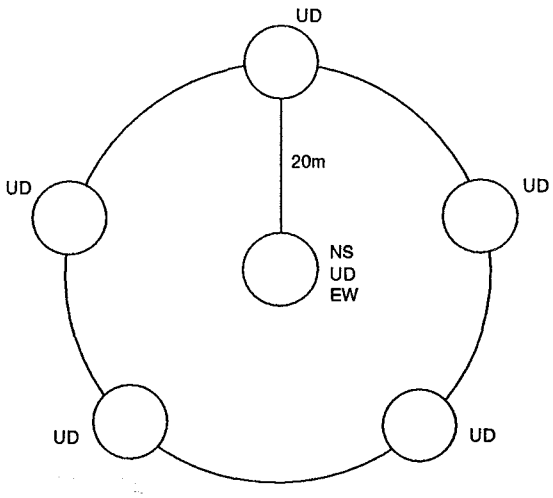

Figure 1. Observed array arrangement for microtremor measurement

Soil profile

For all the sites under study, at least one type or both types of geological investigations (i.e., SPT and PS-logging) exist. For six sites PS-logging exist. These are obtained from in-situ measurements. Figure 3a shows measured PS-logging for the sites.

For seven other sites there exist only SPT

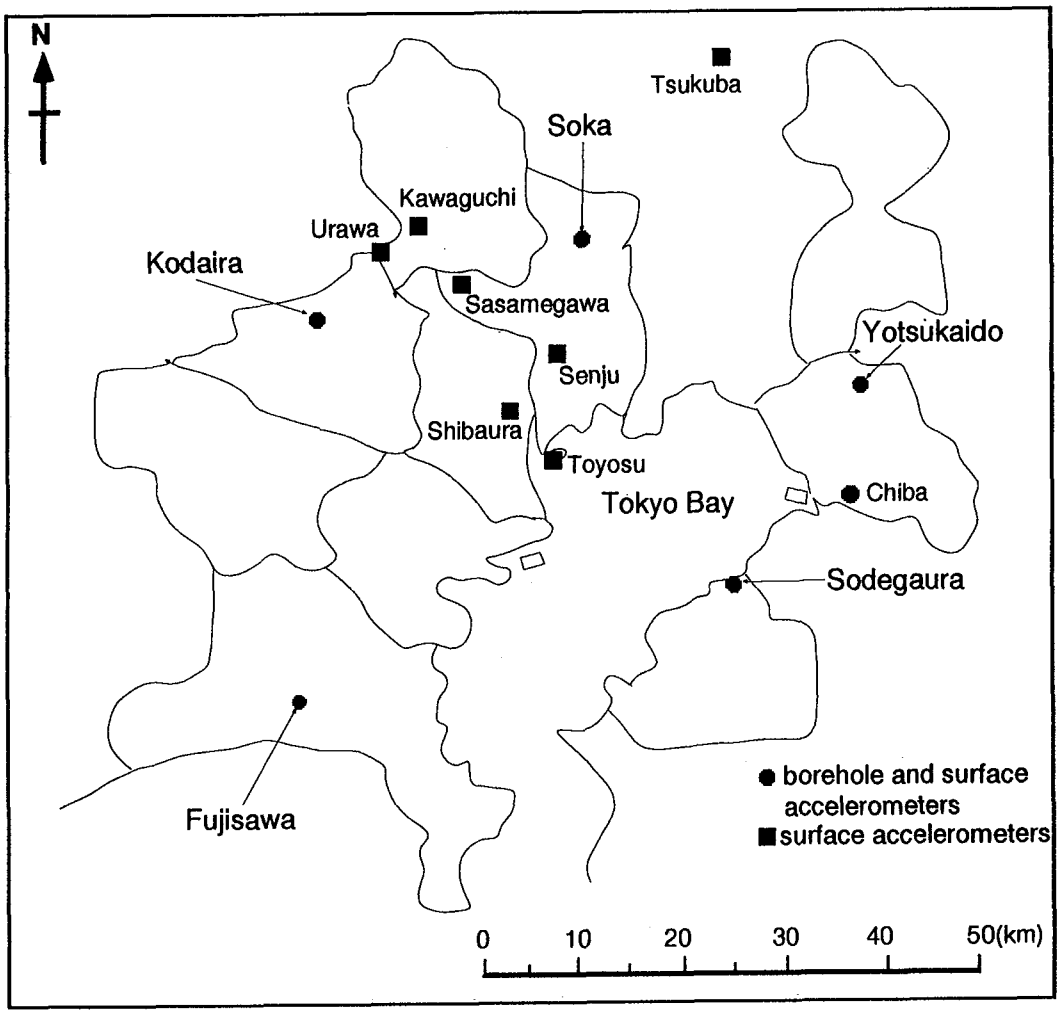

Figure 2. Earthquake observation stations under study

Table 1. Basic information related to microtremor measurements

Site	Date mm/dd/yy	Duration (hour)	Weather condition	Type of measurements	Shear wave velocity
1. Chiba	03/15/93	24	sunny	array	measured
2. Fujisawa	11/04/93	24	sunny	point	measured
3. Shibaura	06/28/94	1	cloudy	point	estimated
4. Kawaguchi	08/15/94	1	sunny	point	estimated
5. Kodaira	11/25/93	24	sunny	array	measured
6. Sasamegawa	08/15/94	1	sunny	point	estimated
7. Senju	08/15/94	1	sunny	point	estimated
8. Sodegaura	11/11/93	24	rainy	array	measured
9. Soka	12/09/93	24	sunny	array	measured
10. Toyosu	06/28/94	1	cloudy	point	estimated
11. Tsukuba	09/19/94	1	cloudy	point	estimated
12. Urawa	08/15/94	1	sunny	point	estimated
13. Yotsukaido	11/17/93	24	sunny	point	measured

profile. To convert these data into shear wave velocities the following empirical relationship (Ohta and Goto, 1978) has been used:

$$V_s = 69N^{0.17}D^{0.2}F_1F_2 \qquad (1)$$

where N is the SPT value, D the depth in meters below the ground surface, F_1 equals 1.0 for alluvial deposits and 1.3 for dilluvial deposits, F_2 depends on the grain size: a value of 1.0 for clay, 1.09 for fine sand, 1.14 for coarse sand, 1.15 for gravelly sand and 1.45 for gravel. Equation (1) yields shear wave velocities for the seven sites as shown in Figure 3b.

One point microtremor observation and analytical solution

Fourier spectrum of horizontal and vertical motion

Obtained velocity records are converted from time domain to frequency domain to get the Fourier spectrum and it has been smoothed by using a Parzen window of bandwidth 0.4Hz. Instead of using all the observed time records, six time instants each at 4 hours apart are selected from 24 hour observation for six sites (Table 1), for investigation. Each time instant is at least 20s long.

Figure 4 shows Fourier spectra microtremor observations at the six sites. Figure 4a shows the vertical and horizontal Fourier spectra of microtremors observed at Chiba. The peak value of the spectra lies between 0.2s to 0.4s for both the horizontal and vertical motions for all the 6 time instants.

Figure 4c shows the vertical and horizontal Fourier spectra of microtremors observed at Kodaira. The horizontal motion in the afternoon (8h, 12h and 16h) has a wide peak between 0.2 to 0.4s and in the night (20h, 24h and 4h), it has two peaks around 0.2s and around 0.4s. For vertical motion, there are two peaks, one around 0.1s and another around 0.4s. The peak around 0.4s is comparatively more stable than the peak around 0.1s within a day.

Figure 4d shows the vertical and horizontal Fourier spectra of microtremors observed at Sodegaura. Both spectra are almost stable during a day. Several sharp peaks for all the six time instants can be observed for both spectra especially a peak around 0.1s, where amplitude level is high. This may be due to vibration of machineries in a nearby machine room.

The Fourier spectra (Figure 4e) at Soka are similar to the spectra at Sodegaura, where the change of amplitude level of the spectra at different time instants of a day is comparatively small. Again, for Fujisawa (Figure 4b) and Yotsukaido (Figure 4f), the Fourier spectra are similar to the spectra at Kodaira, where the change of amplitude level of the spectra at different time instants of a day is comparatively large.

Stability of horizontal-to-vertical Fourier spectral ratio

The amplitude ratio calculated in this study is defined by Nakamura (1989). Amplitude ratios of Fourier amplitude spectra of the NS and EW components, respectively, to that of the UD components, $AR_{NS}(T)$ and $AR_{EW}(T)$, are obtained as follows:

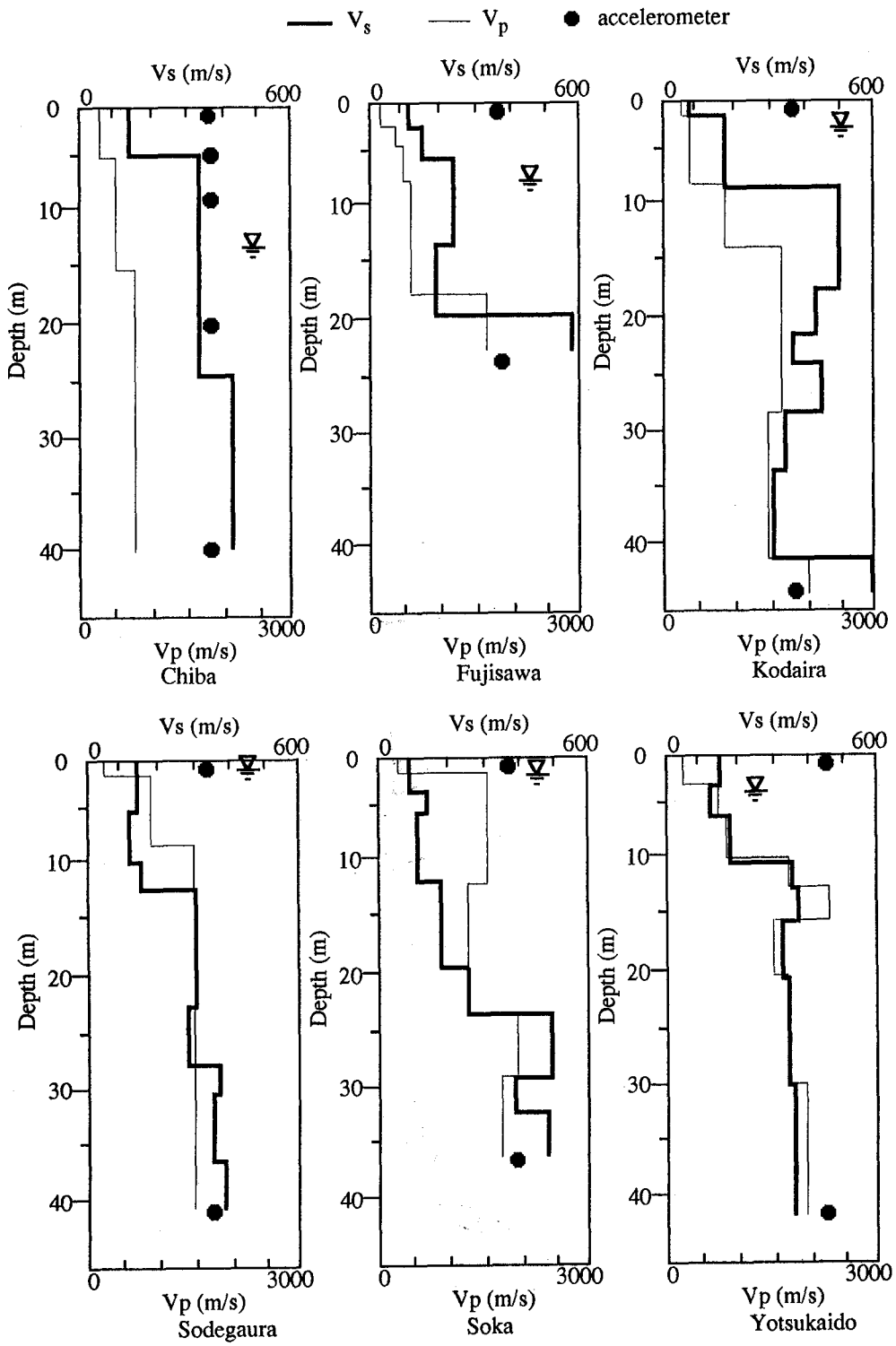

Figure 3a. Measured underground structures of the six sites

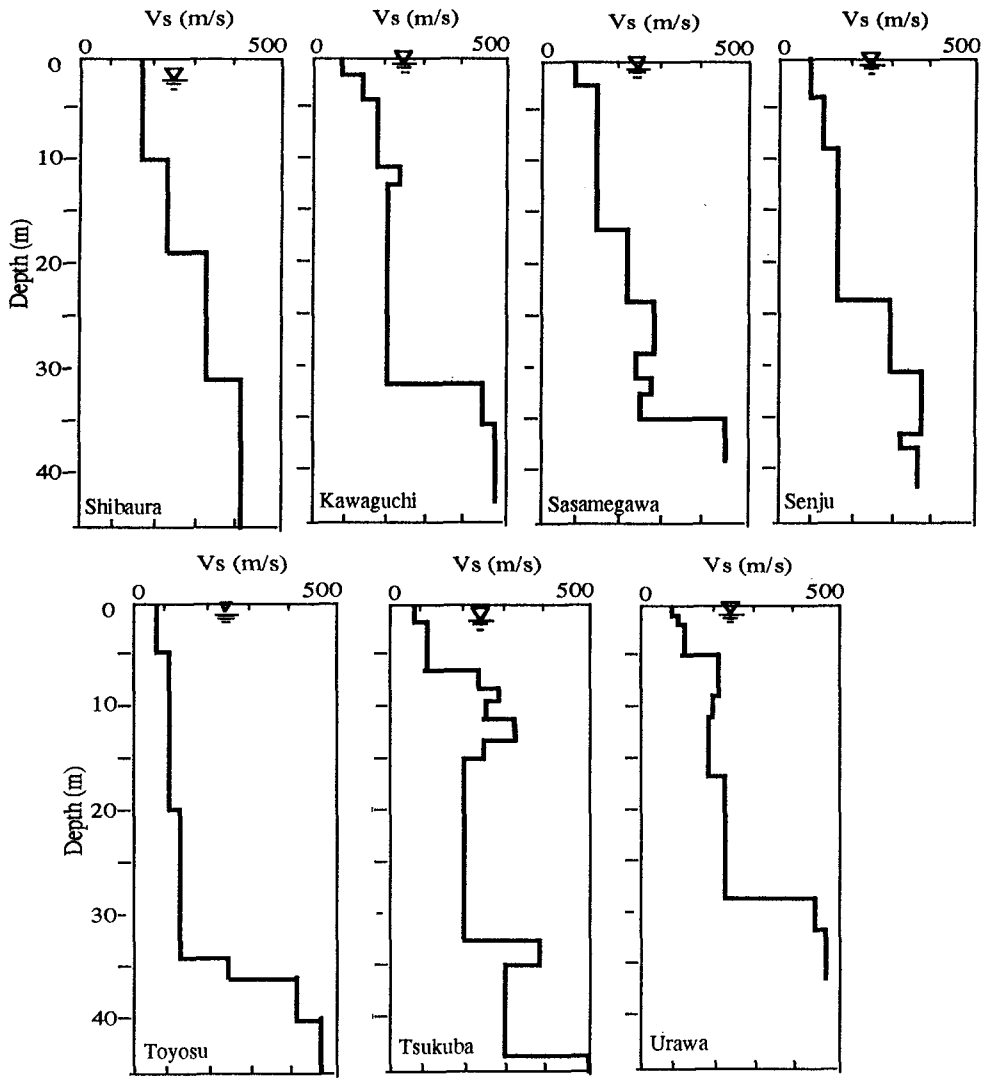

Figure 3b. Estimated underground structures of the seven sites

$$AR_{NS}(T)=\frac{F_{NS}(T)}{F_{UD}(T)} \qquad AR_{EW}(T)=\frac{F_{EW}(T)}{F_{UD}(T)} \tag{2}$$

where $F_{NS}(T)$, $F_{NS}(T)$ and $F_{UD}(T)T$ is the Fourier amplitude spectra in the NS, EW and direction, $F_{EW}(T)$ the Fourier amplitude spectrum in the EW direction and $F_{UD}(T)$ the Fourier amplitude spectrum in the NS, EW and UD directions, respectively.

In Figure 5, amplitude ratios, $AR_{NS}(T)$ and $AR_{EW}(T)$ of the Fourier spectra of two horizontal components, are shown for six time instants at the six sites. The characteristics of the preak periods for the amplitude ratios are different from those for Fourier spectra. Although Fourier spectra at Kodaira and Yotsukaido are not so stable with time, the amplitude ratios at different time instants of a day are stable for all the six sites. Especially the Fourier spectra for Sodegaura show a peak around

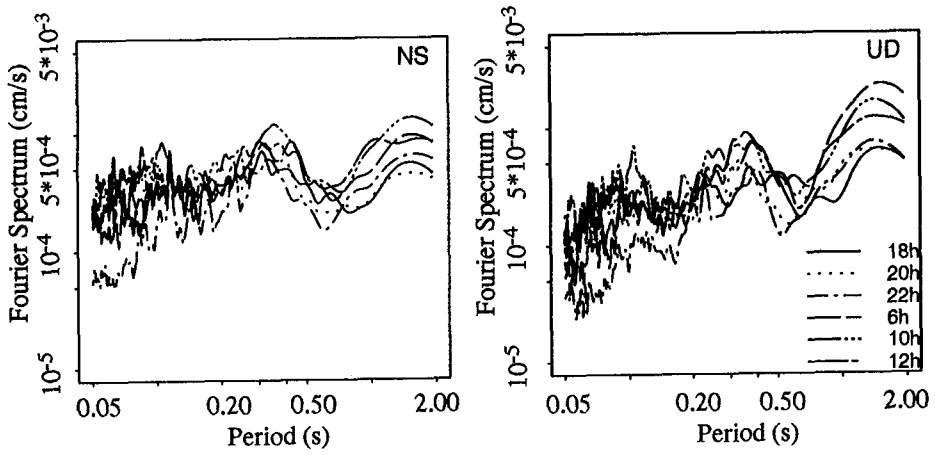

(a) Chiba

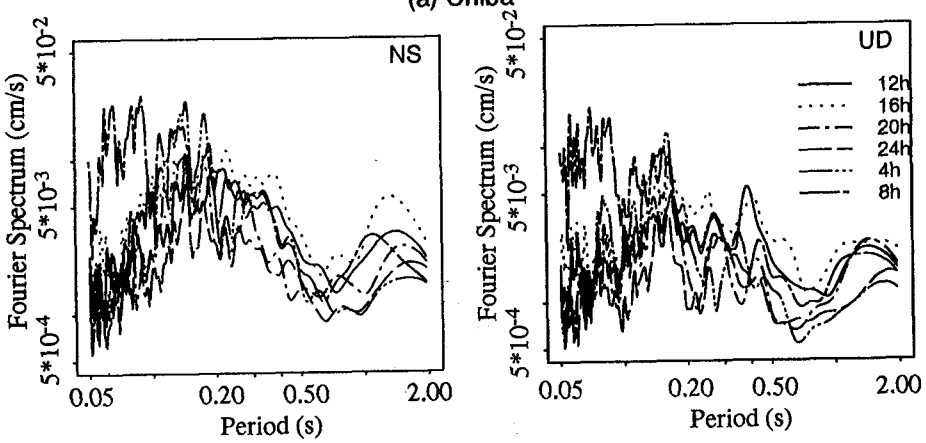

(b) Fujisawa

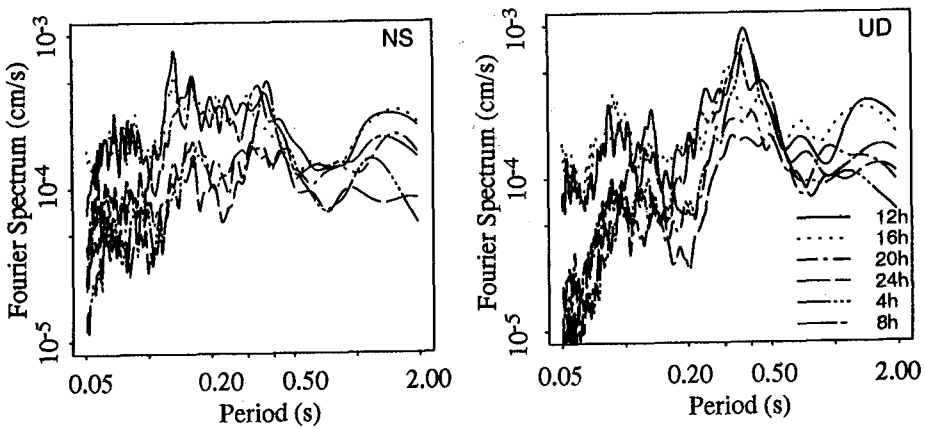

(c) Kodaira

Figure 4 Horizontal and vertical Fourier spectra of microtremors at the six sites

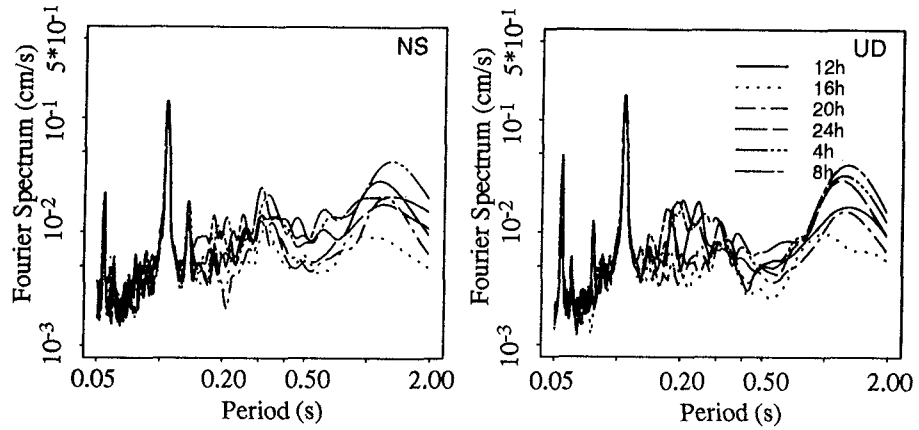

(d) Sodegaura

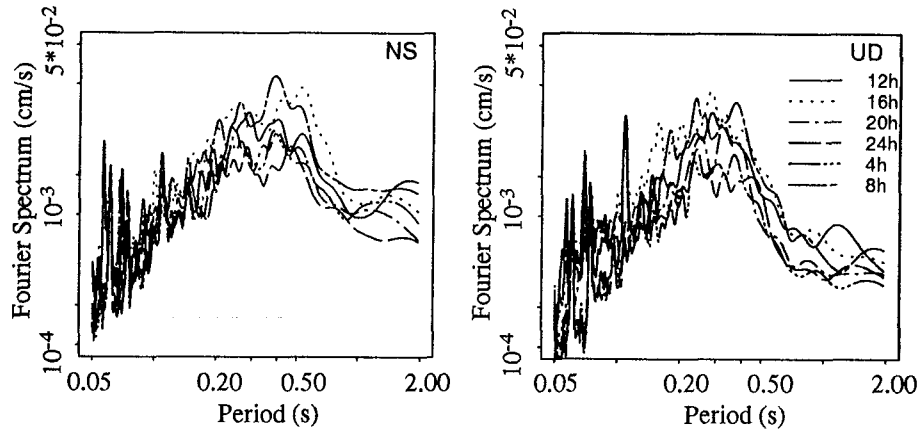

(e) Soka

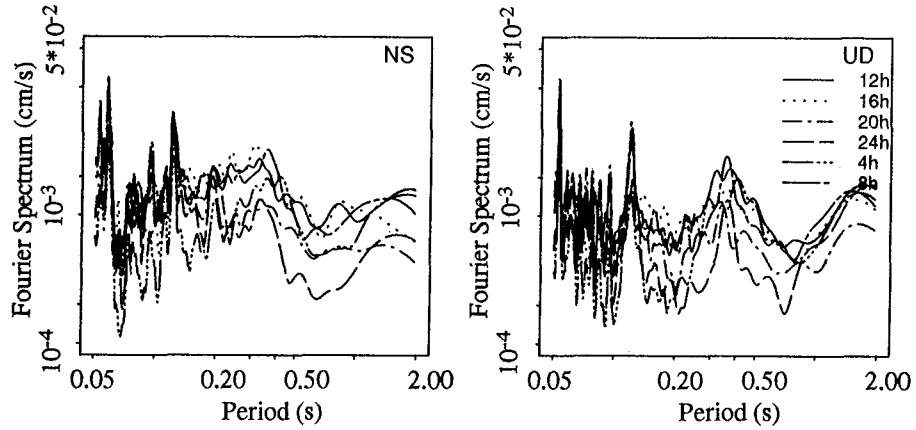

(f) Yotsukaido

Figure 4 (contd.) Horizontal and vertical Fourier spectra of microtremors at the six sites

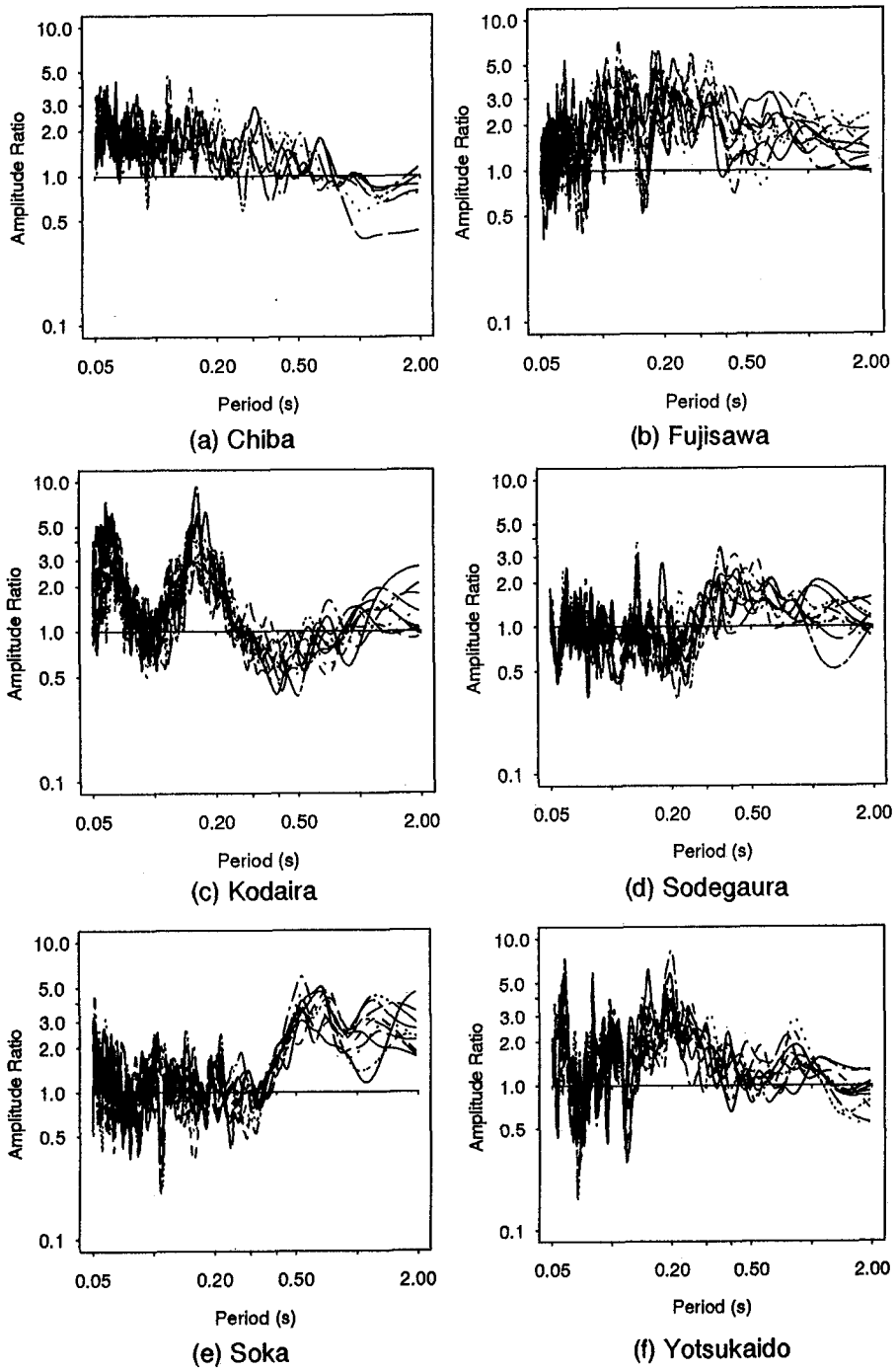

Figure 5 Microtremor amplitude ratios at the six sites for several time instants (NS and EW)

0.1s probably due to the machine vibration but for the amplitude ratio that peak can not be observed. From these facts, it can be concluded that the amplitude ratio is less influenced by the source of vibration than the Fourier spectrum of any direction and may reflect the particular characteristics of the site.

Comparison between observed and analytical amplitude ratios

From the existing borelogs and PS-loggings (Figure 3), soil model at each site is established for theoretical analysis. The transfer function of the shear-wave (the surface motion versus the incidental motion at some depth) and the amplitude ratio for the fundamental mode of Rayleigh-wave were calculated at the sites using those soil models. For the calculation of transfer function of shear-wave, a damping ratio of 2% has been used, assuming input motion at the outcrop.

Figure 6 shows the transfer function of shear-wave, amplitude ratios of Rayleigh-wave and microtremor for thirteen sites. During comparison with the theoretical curves, the amplitude ratio, $AR(T)$, of microtremor used can be expressed by the following equation:

$$AR(T)=\frac{\sqrt{F_{NS}(T)F_{EW}(T)}}{F_{UD}(T)} \tag{3}$$

where $F_{NS}(T)$, $F_{EW}(T)$ and $F_{UD}(T)$ are average Fourier spectra of six time instants.

The trend of three curves, i.e., two theoretical and one observed, somewhat resembles each other for these sites. Especially in between the amplitude ratios of Rayleigh-wave and microtremor observation, the period at which the Rayleigh-wave amplitude ratio either suddenly drops or peaks, microtremor amplitude ratio closely resembles it. In a general sense, amplitude ratio for pure Rayleigh-wave is always lower than the amplitude ratio of microtremor. The reason is that microtremor may contain some shear-wave and Love-wave contents as well as Rayleigh-wave. Further explanation for this kind of behavior can be found from the parametric study of two layer soil model.

Two layer soil model

To investigate the reason behind the similarity between the period corresponding to the peak amplitude ratio of the Rayleigh-wave and predominant period of shear-wave transfer function, a parametric study is conducted using a two-layer soil model. Five cases of H/V_{s1} ratio are considered, where H and V_{s1} are the thickness and shear-wave velocity of the surface layer, respectively. The five cases are actually five predominant periods of shear-wave ($T_s=4H/V_{s1}$) namely, 0.25s, 0.5s, 0.75s, 1.0s and 1.5s. The impedance ratio (α) is approximately defined as the ratio between the shear wave velocity at the surface layer (V_{s1}) and at the base layer (V_{s2}) is changed for investigation. Table 2 shows different parameters used for two-layer soil model for $T_s=1s$. In this study, for the surface layer: Poisson ratio equal to 0.49 and density equal to 1.8tf/m^3 and for the base layer: Poisson ratio equal to 0.40, density equal to 2.0tf/m^3 and V_{s2} equal to 500m/s are assumed. Figure 7 shows relation between amplitude ratio of Rayleigh-wave and period for different impedance ratios for $T_s=1s$. Figure 8 explains different shape of the Rayleigh-wave amplitude ratio curves after Ohmachi et al. (1994). Depending on the movement of particle (i.e., either retrograde or prograde movement) in the Rayleigh-wave as shown, curves of Figure 7 can be categorized into three types. Type 1 which covers low impedance range,

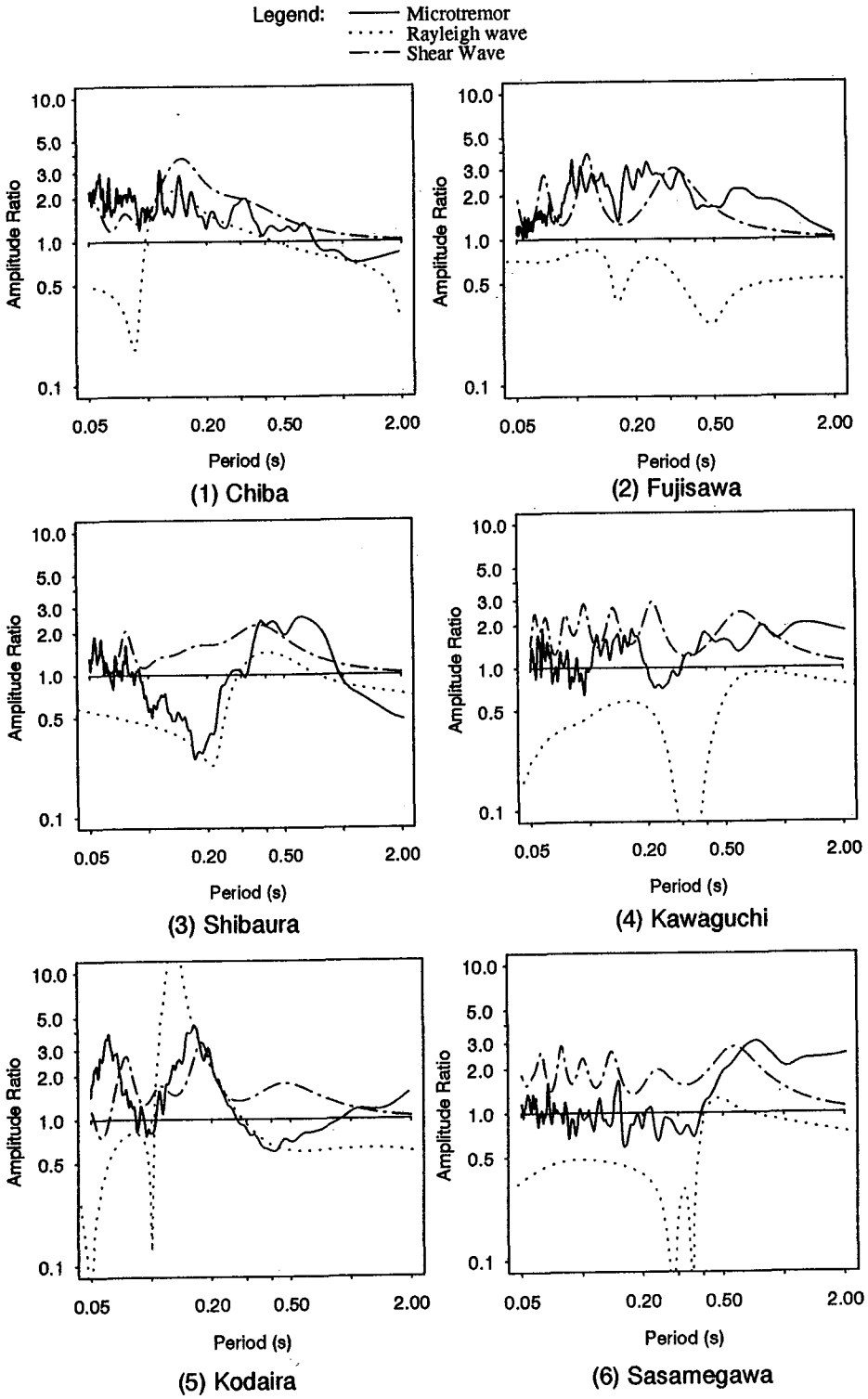

Figure 6. Amplitude ratios of microtremor and theoretical Rayleigh-wave plotted with transfer function of shear-wave

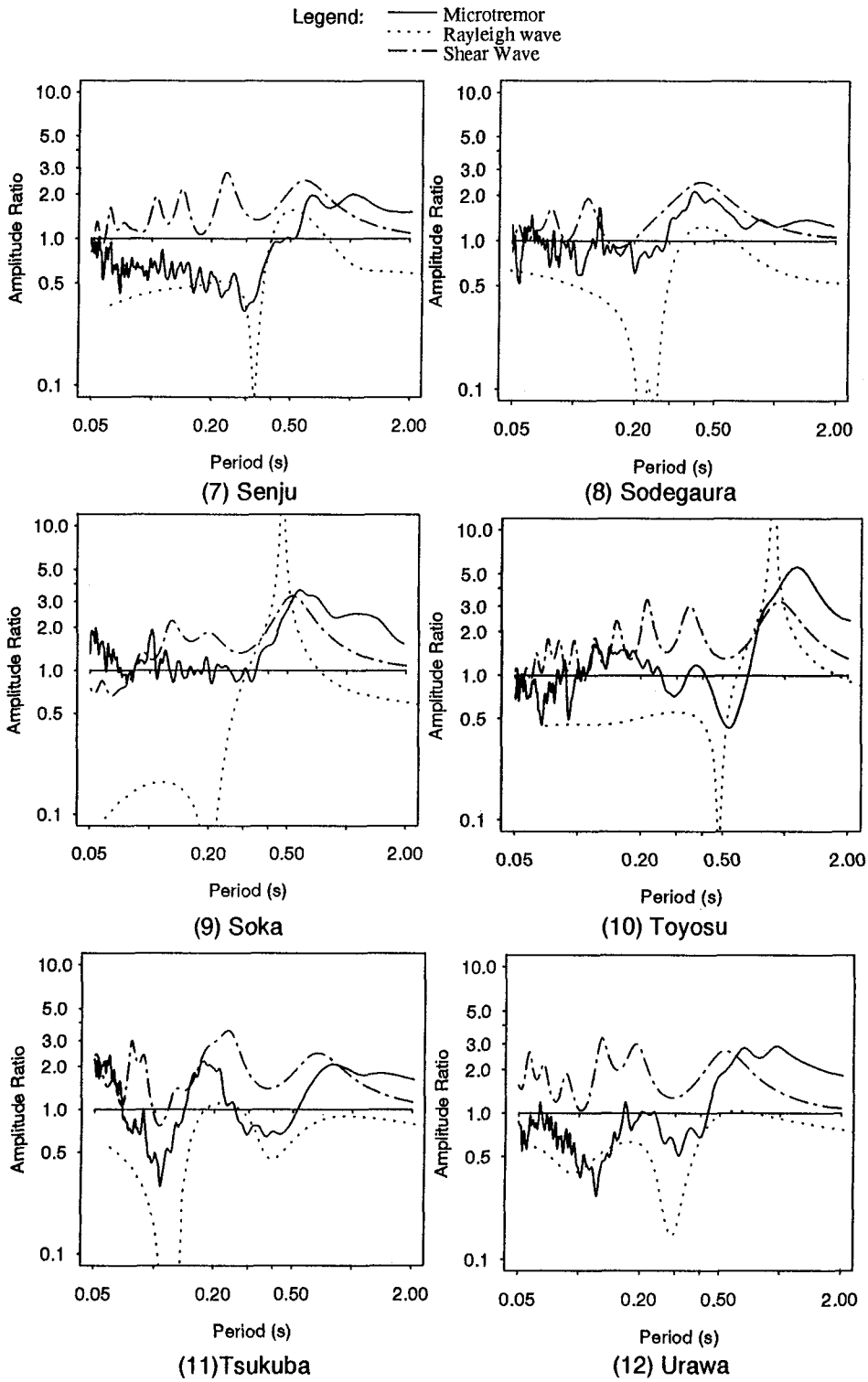

Figure 6 (contd.). Amplitude ratios of microtremor and theoretical Rayleigh-wave plotted with transfer function of shear-wave

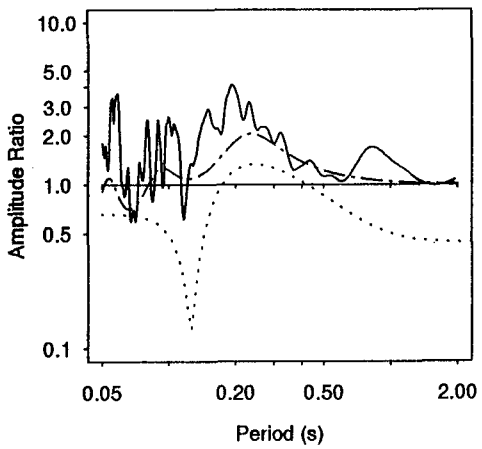

(13) Yotsukaido

Figure 6 (contd.). Amplitude ratios of microtremor and theoretical Rayleigh-wave plotted with transfer function of shear-wave

Table 2. Two-layer soil model

Case	Impedance Ratio ($\alpha=V_{s1}/500$)	Shear-wave Velocity of Surface Layer V_{s1}(m/s)	Thickness of Surface Layer (T_s=1s) H(m)	Modulus of Elasticity (kgf/m^2)
1	1.00	500.00	125.00	1.3410
2	1.25	400.00	100.00	0.8582
3	1.50	333.33	83.33	0.5960
4	1.75	285.71	71.43	0.4379
5	2.00	250.00	62.50	0.3353
6	2.15	232.60	58.15	0.3062
7	2.20	227.27	56.82	0.2925
8	2.25	222.22	55.60	0.2649
9	2.50	200.00	50.00	0.2146
10	2.65	188.68	47.17	0.2016
11	2.90	172.41	43.10	0.1683
12	3.00	166.67	41.67	0.1490
13	3.25	153.85	38.46	0.1270
13	3.50	142.86	35.72	0.1095
14	3.75	133.33	33.33	0.0954
15	4.00	125.00	31.25	0.0838
16	4.25	117.65	29.41	0.0742
17	4.50	111.11	27.78	0.0662
18	5.00	100.00	25.00	0.0536
19	5.50	90.91	22.73	0.0443
20	6.00	83.33	20.83	0.0372
21	6.50	76.92	19.23	0.0317
22	7.00	71.43	17.86	0.0274
23	8.00	62.50	15.63	0.0210

contains only retrograde movement. In this case, trough can be seen for the amplitude ratio of Rayleigh-wave if the impedance ratio becomes larger than about 2. Type 2 which covers mid-range of impedance, contains both retrograde and prograde movements as well as sharp troughs. Here, the transition zone between Type 2 and Type 3 is around the impedance ratio 2.9. Type 3 which covers range where impedance ratio is generally greater than 3, contains both retrograde and prograde movements as well as sharp troughs and sharp peaks.

Figure 9 shows the relationship between period ratio (T_r/T_s) and impedance ratio of the two layers, where T_r is the period corresponding to the peak amplitude ratio of Rayleigh-wave. From this figure it is clear that Type 2 and Type 3 has a clear transition point around an impedance ratio of 2.9, for all the five cases of T_s. For these five values of T_s, the predominant period of Rayleigh-wave amplitude ratio approaches the predominant period of shear-wave around impedance ratio of 4.5.

The appearance of sharp peak of the Rayleigh-wave amplitude ratio at Kodaira and Soka may be attributed to comparatively large contrast between the surface and base layer at those sites. On the other hand, absence of sharp peak of the Rayleigh-wave amplitude ratio at Chiba, Sodegaura and Yotsukaido may be attributed to the lack of contrast at those sites. The contrasts of ground at some sites, such as Fujisawa, are comparatively large but the correspondence between the amplitude ratio of Rayleigh-wave and shear-wave is not good. It is possible to explain most of the multi-layer phenomena related to amplitude ratio of Rayleigh-wave with the two-layer model but a case like Fujisawa is difficult to explain. One of the possible reason may be explained by the fact that only shallow soil profile is known at this site. The possible change in deeper soil layers may cause difference in the dispersion curve.

Microtremor observation by array

Generally, two estimation methods have been used for the frequency wave-number (F-K) analysis of array data with non-uniform distances between neighboring sensors. One is the frequency domain beam-forming method (BFM) by Lacoss et al. (1969), and the other is the maximum likelihood method (MLM) by Capon (1969). In this study, MLM method has been used. The estimate of the F-K spectrum $P(f,k)$ is given by

$$P(f,k) = \sum_{l,m=1}^{n} A_l^*(f,k) A_m(f,k) \phi_{lm}(f) \exp\{ik(X_l - X_m)\} \tag{4}$$

where

$$A_j(f,k) = \sum_{l=1}^{n} (\phi_{jl}(f) \exp\{ik(X_j - X_l)\})^{-1} / \sum_{j,l=1}^{n} (\phi_{jl}(f) \exp\{ik(X_j - X_l)\})^{-1}$$

In equation (6), f is the frequency, $\boldsymbol{k}$ is the two-dimensional horizontal-wavenumber vector, n is the number of sensors. The symbol $\phi_{lm}(f)$ is the estimate of the cross-power spectrum between l-th and the m-th data, and X_l and X_m are the coordinates of the l-th and the m-th sensors, respectively.

Dispersion characteristics of vertical motion

The frequency-wavenumber (F-K) spectrum analysis is conducted using microtremors observed at Kodaira, Sodegaura and Soka. At these sites, array networks have been extended for the vertical motion. From the peak location of frequency-wavenumber space as shown in Figure 10 for Kodaira site, apparent velocity (c) and azimuthal angles (θ) have been calculated using the following equations:

$$c = 2\pi f / \sqrt{k_{xo}^2 + k_{yo}^2} \tag{5}$$

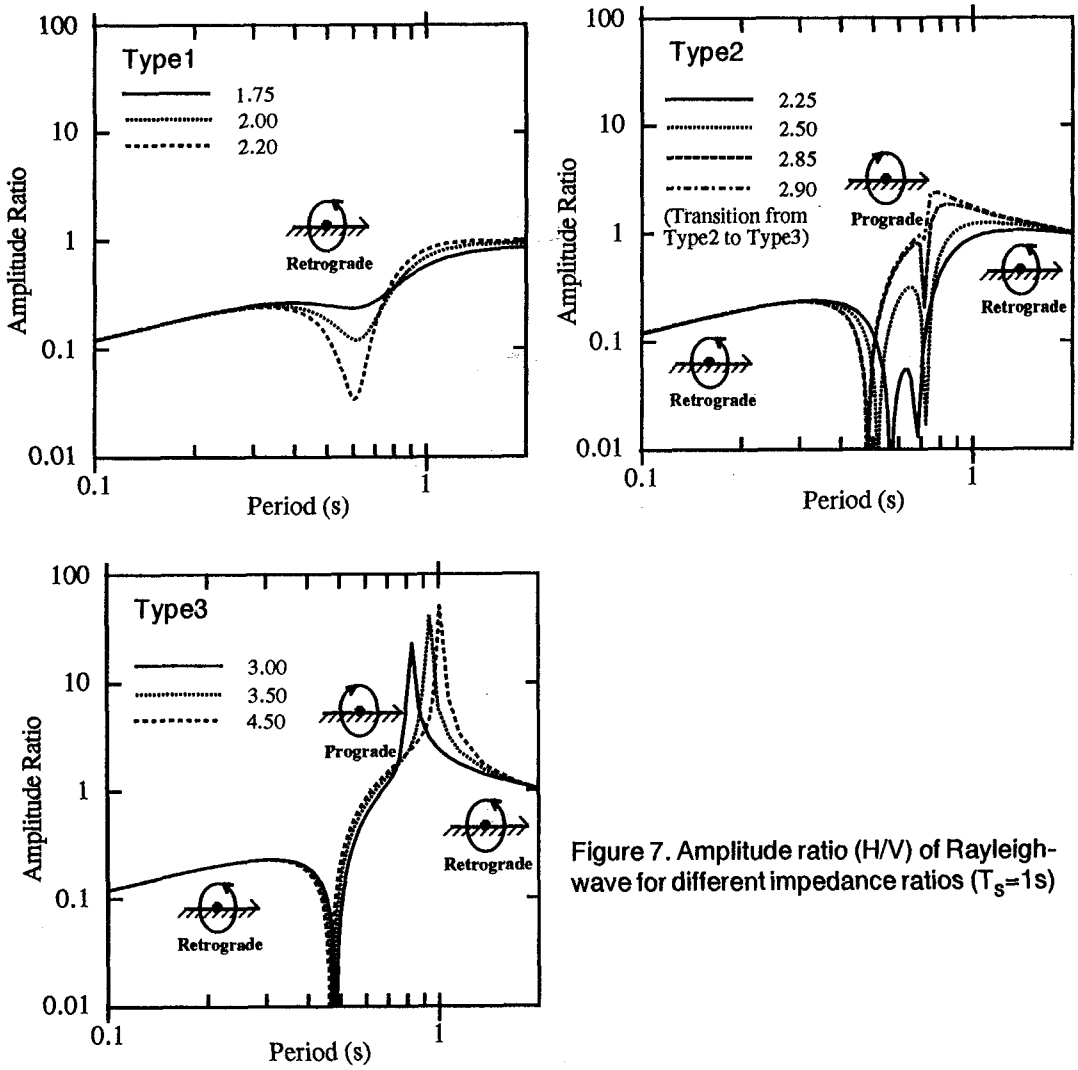

Figure 7. Amplitude ratio (H/V) of Rayleigh-wave for different impedance ratios (T_S=1s)

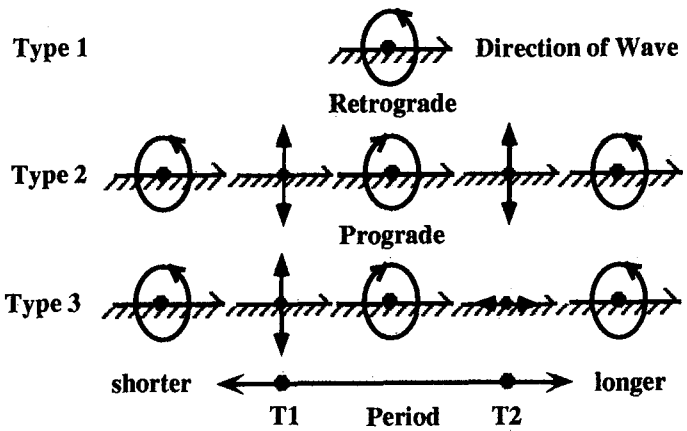

Figure 8. Categorization of ground based on the particle orbit of fundamental mode of Rayleigh-wave (Ohmachi et al., 1994)

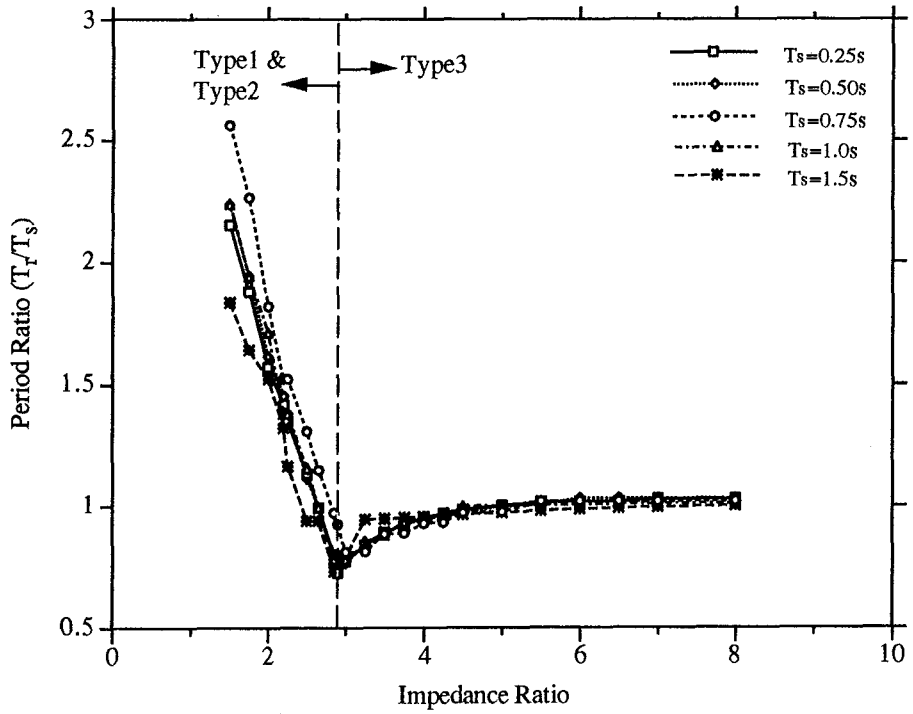

Figure 9. Relationship between impedance ratio and period ratio (T_r/T_s) of Rayleigh and Shear-waves

$$\theta = \tan^{-1}\left(\frac{k_{xo}}{k_{yo}}\right) \tag{6}$$

where f is the central frequency of the Parzen window, $\boldsymbol{k}=[k_{xo},k_{yo}]^T$ represents the peak of the F-K spectrum and θ is defined clockwise from the north (k_y).

Figures 11 shows the apparent velocity of vertical motions of microtremors for six time instants together with the theoretical dispersion curves of the phase velocity of the Rayleigh-wave at the three array sites. This figures also show propagation direction of vertical motions of observed microtremors measured clockwise from the north for the six time instants.

Kodaira: Although Fourier spectra at Kodaira change for each time instant within a day, the propagation velocity is relatively stable. The range of period for which dispersive characteristics of microtremor is obtained is thought to be dominated by Rayleigh-wave. Roughly the waves are coming from north (0°) to east (90°). The reason may be explained by the fact that the Shin-Ome highway is situated in this direction, which has heavy traffic both in the day and night time. The vertical motion is thought to be generated mainly by this traffic.

Sodegaura: Fourier spectra of vertical motion at Sodegaura for different time instants within a day are comparatively more stable than those at Kodaira. At a period around 0.1s, Fourier spectrum has a large peak for the three microtremor components and high phase velocity can be observed in Figure 11b. This is thought due to a noise which is coming from the southwest direction along the whole day. A machine facility is working several tens of meters away from this location round the clock and can be heard

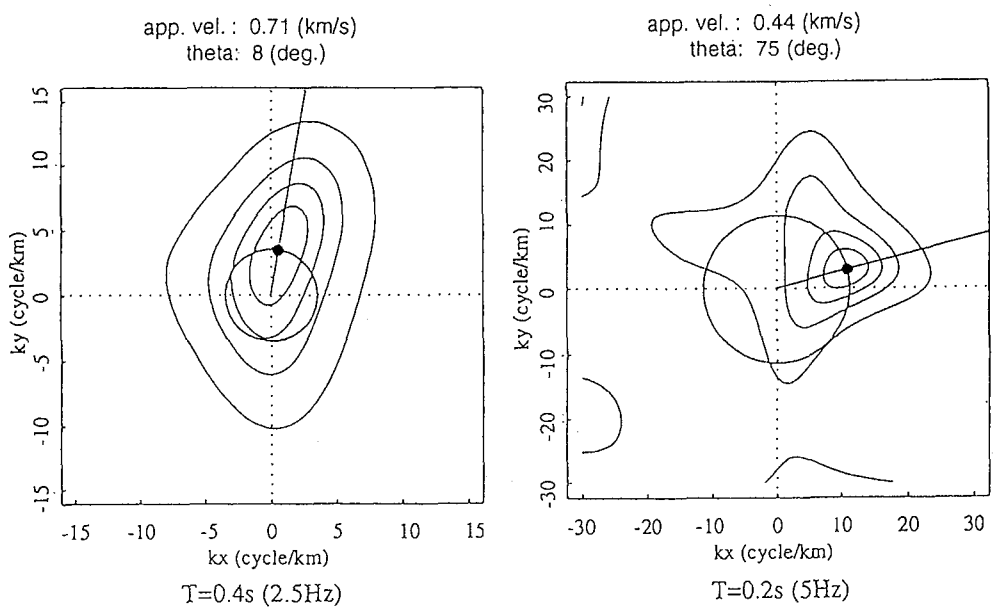

Figure 10. FK-spectrum for two particular frequencies (Kodaira)

clearly from the site. The large value of phase velocity may be attributed to the influence of body wave, which does not decrease much due to short separation distance between the measuring point and the source. For the other period range it is thought that waves are propagating mainly from the southeast direction.

Soka: Like Sodegaura, the Fourier spectrum of the vertical motion at Soka changes little with different time instants within a day. The apparent phase velocities are comparatively stable. Except the data at period 0.2s, the dispersion characteristic of propagation velocity corresponds well with the theoretical dispersion characteristic of the Rayleigh-wave. A peak around 0.2s can be observed in the vertical component of Fourier spectrum at this site. At this period, a stable noise is coming roughly from the north as can be observed from Figure 11c. A round the clock industrial plant is operating in this direction. The vibration level of this plant is not as clear as Sodegaura but it can be heard and propagation direction can be identified. Similar to Sodegaura, the phase velocity around this period may be attributed to the influence of body wave and may have attenuated due to the distance traversed between the source and the measuring point. The propagation directions for other period ranges are scattered. The volume of traffic near this site is small. From the different observed waves propagating from various directions, the wave coming from the nearby plant is thought to be the principal one among the artificial sources.

Conclusions

Short-period microtremor observations have been performed at 13 sites in Tokyo metropolitan area. The amplitude ratio of Fourier spectra defined by Nakamura (1989) has been used for site amplification characterization. At three out of six sites where triaxial accelerometers are located, theoretical dispersion curves are compared with apparent phase velocity obtained from microtremor observations

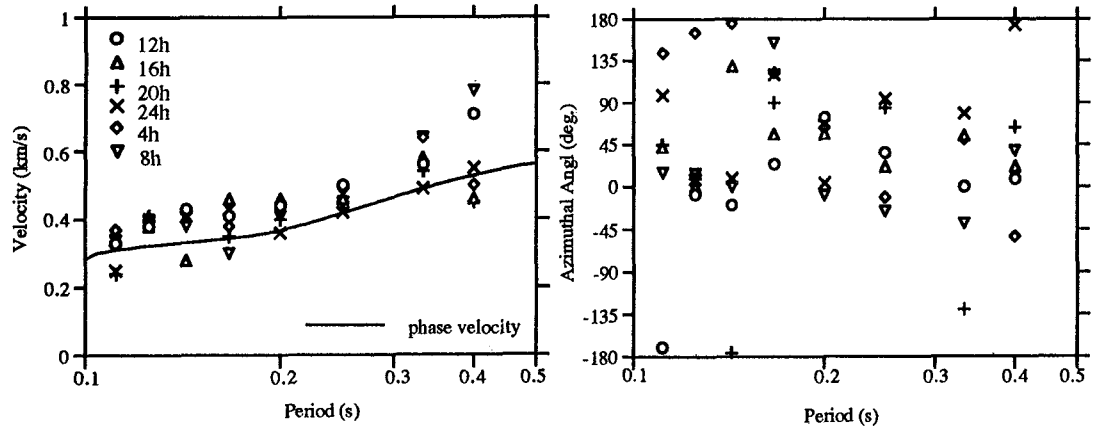

(a) Kodaira

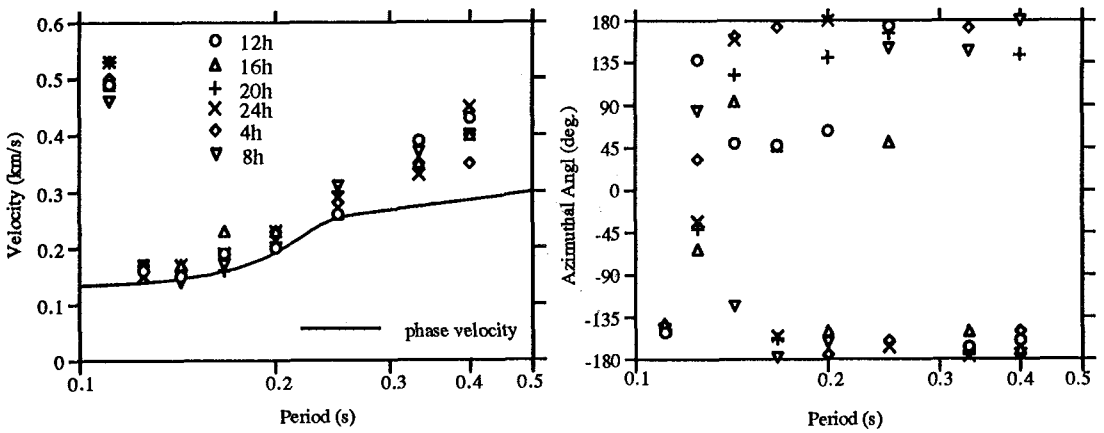

(b) Sodegaura

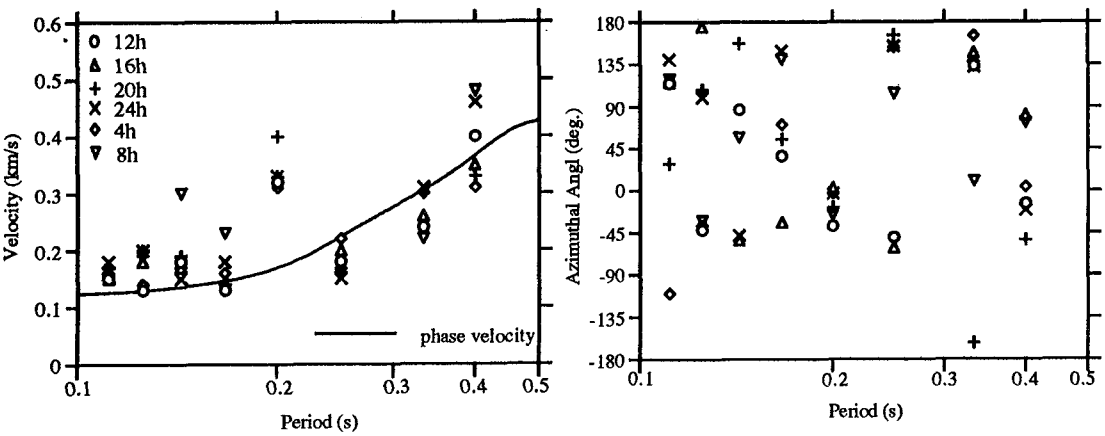

(c) Soka

Figure 11. Apparent velocity of microtremors and dispersion curve of Rayleigh-wave (left) and azimuthal angles of microtremors (right) for six time instants

by array. Following conclusions are drawn from this study:

The Fourier spectra of horizontal and vertical components of microtremors show variations with time, but their ratio is stable for different time instants. The characteristics of the microtremor's amplitude ratio are similar to that of Rayleigh-wave and the period corresponding to the peak amplitude ratio corresponds to the peak periods of Rayleigh-wave amplitude ratio and shear-wave transfer function.

A parametric study for two-layer soil model reveals that the period corresponding to the peaks for Rayleigh-wave and shear-wave are close for ground having large impedance ratio.

The propagation velocity obtained from the frequency-wavenumber spectrum analysis of vertical motion of observed microtremors is in good agreement with the phase velocity of Rayleigh-wave. Also, the azimuthal angles at different periods determine the directions of microtremor sources.

References

Aki, K. (1957). Space and time spectra of stationary stochastic waves, with special reference to microtremors, *Bull. of earthquake research institute* **35**, 415-456.

Capon, J. (1969). High-resolution frequency-wavenumber spectrum analysis, *Proc. IEEE* **57**, 1408-1418.

Field, E. H. and K. H. Jacob (1995). A comparison and test of various site-response estimation techniques, including three that are not reference-site dependent, *Bull. seism. soc. Am.* **85**, 1127-1143.

Kanai, K. and T. Tanaka (1961). On microtremor VIII, *Bull. of earthquake research institute* **39**, 97-114.

Lacoss, R. T., E. J. Kelly, and M. N. Toksoz (1969). Estimation of seismic noise structure using array, *Geophysics* **34**, 21-38.

Lachet, C. and P. Y. Bard (1995). Theoretical investigations on the Nakamura's technique, *Proc. 3rd int. conf. on recent advances in geotechnical earthquake eng. and soil dyn.* **II**, 671-675.

Lermo, J. and F. J. Chavez-Garcia (1994a). Are microtremors useful in site response evaluation, *Bull. seism. soc. Am.* **84**, 1350-1364.

Lermo, J. and F. J. Chavez-Garcia (1994b). Site effect evaluation at Mexico city: dominant period and relative amplification from strong motion and microtremor records, *Soil dyn. earthquake eng.***13**, 413-423.

Ohmachi, T., K. Konno, T. Endoh and T. Toshinawa (1994). Refinement and application of an estimation procedure for site natural periods using microtremor, *J. civil eng., JSCE* **489(I-27)**, 251-260 (in Japanese).

Ohta, Y. and N. Goto (1978). Empirical shear wave velocity equations in terms of characteristics soil indexes, *Earth. Eng. Struct. Dyn.*, **6**, 167-187.

Nakamura, Y. (1989). A method for dynamic characteristics estimation of subsurface using microtremor on the ground surface, *QR of RTRI* **30**, 25-33.

Sato, T., H. Kawase, M. Matsui,.and S. Kataoka (1991). Array measurement of high-frequency microtremors for underground structure estimation, *Proc. 4th int. conf. on seismic zonation* **II**, 409-416.

Suzuki, T., Y. Adachi, and M. Tanaka (1995). Application of microtremor measurements to the estimation of earthquake ground motions in Kushiro city during the Kushiro-oki earthquake of 15 January 1993, *Earthq. eng. struct. dyn.* **24**, 595-613.

Tamura, T., O. Nagai, H. Kokubo, and H. Sumita (1993). Characteristics of wave group of microtremors obtained by array measurement, *J. struct. consr. eng, AIJ* **449**, 83-91 (in Japanese).

Theodulidis, N. P. and P. Y. Bard (1995). Horizontal to vertical spectral ratio and geological conditions: an analysis of strong motion data from Greece and Taiwan (SMART-1), *Soil dyn. earthquake eng.* **14**, 177-197.

Tokimatsu, K. and Y. Miyadera (1992). Characteristics of Rayleigh waves in microtremors and their relation to underground structures, *J. struct. consr. eng, AIJ* **439**, 81-87 (in Japanese).

Tokimatsu, K., Y. Nakajo, and S. Tamura (1994). Horizontal-to-vertical amplitude ratio of short-period microtremors and its relation to site characteristics, *J. struct. consr. eng, AIJ* **457**, 11-18 (in Japanese).

Wakamatsu, K. and Y. Yasui (1995). Possibility of estimation for amplification characteristics of soil deposits based on ratio of horizontal to vertical spectra of microtremors, *J. struct. consr. eng, AIJ* **471**, 61-70 (in Japanese).

Yamazaki, F., T. Katayama, and Y. Yoshikawa (1994). On-line damage assessment of city gas networks based on dense earthquake monitoring, *Proc. 5th U.S. nat. conf. on earthquake eng.* **IV**, 829-837.

Yoshikawa, Y., H. Kano, F. Yamazaki, T. Katayama, and N. Akasaka (1995). Development of SIGNAL: An early warning system of city gas network, *Proc. 4h U.S. conf. on lifeline earthquake eng.*,160-167.